

Dynamic Approach to the Fully Frustrated XY Model*

H.J. Luo, L. Schülke and B. Zheng*

Universität – GH Siegen, D – 57068 Siegen, Germany

* Universität Halle, D – 06099 Halle, Germany

Using Monte Carlo simulations, we systematically investigate the non-equilibrium dynamics of the chiral degree of freedom in the two-dimensional fully frustrated XY model. The critical initial increase of the staggered chiral magnetization is observed. By means of the short-time dynamics approach, we estimate the second order phase transition temperature T_c and all the dynamic and static critical exponents θ , z , β and ν .

PACS: 64.60.Cn, 75.10.Hk, 64.60.Ht, 75.40.Mg

For critical phenomena, it is traditionally believed that universal behaviour exists only in equilibrium or in the long-time regime of the dynamical evolution. The universal scaling behaviour is described by a number of critical exponents. Due to critical slowing down, numerical measurements of the critical exponents are very difficult.

Recently, much progress has been achieved in dynamic critical phenomena. It was discovered that, already after a microscopic time scale t_{mic} , universal scaling behaviour emerges in the *macroscopic short-time regime* of the dynamic process [1–6]. To illustrate this, we consider the following dynamic relaxation process: a magnetic system initially in a high-temperature state with a small initial magnetization m_0 is quenched to the critical temperature T_c without an external magnetic field and then released to a dynamic evolution with model A dynamics [7]. At the onset of the evolution, the magnetization is subjected to the scaling form [1,4,5,8,9]

$$M(t, \tau, m_0) \sim m_0 t^\theta F(t^{1/\nu z} \tau). \quad (1)$$

The exponent θ is a new independent exponent, $\tau \sim (T - T_c)/T_c$ is the reduced temperature, β and ν are the static critical exponents, and z is the dynamic exponent. At the critical temperature, $\tau = 0$, the magnetization undergoes a *critical initial increase* $M(t) \sim t^\theta$.

In fact, the short-time dynamic scaling is very general. Another important example is the dynamic relaxation of a magnetic system starting from an ordered state ($m_0 = 1$) [10,9,11,6]. The scaling form for this dynamic process is given by

$$M^{(k)}(t, \tau, L) = b^{-k\beta/\nu} M^{(k)}(b^{-z} t, b^{1/\nu} \tau, b^{-1} L), \quad (2)$$

where, for later convenience, a system with finite size L has been considered. This finite size scaling has the same form as in the long-time regime but is assumed valid in the macroscopic short-time regime.

One of the most prominent properties of the scaling forms (1) and (2) is that the exponents β , ν and z take the same values as in equilibrium or in the long-time regime of the dynamic evolution. It has been suggested that it is possible to determine not only the dynamic but also all the *static* exponents as well as the *critical temperature* already in the short-time regime [5,9] (see also Refs. [11–13,6]). The method may be an alternative way for overcoming critical slowing down since the measurement does not enter the long-time regime. It is important to systematically verify this application in general and complex models.

The two-dimensional fully frustrated XY (FFXY) model has been the topic of many recent studies [14–22]. Critical properties of this model are rather unconventional. On the square lattice, the model has two kinds of phase transitions, i.e. the Kosterlitz-Thouless phase transition (XY-like) and the second order phase transition (Ising-like). Numerical simulations of the FFXY model suffer severely from critical slowing down. Due to the frustration, the standard cluster algorithm does not apply to the FFXY model. Most of the recent work on FFXY models supports that these two phase transitions take place at two different temperatures, however, their critical properties are still not very clear. For example, for the second order phase transition the estimated values of the exponents β and ν differ in the literature [22,21,18,17] and the critical dynamics has not been investigated. It is still a matter of controversy whether the chiral degree of freedom of the FFXY model is in the same universality class as the Ising model [23,22,21,24,25].

In this letter we present results of systematic Monte Carlo simulations for the short-time dynamic behaviour of the second order phase transition in the two-dimensional FFXY model. We confirm the short-time dynamic scaling. For the first time, we confidently determine the dynamic exponents θ and z . Based on the

*Work supported in part by the Deutsche Forschungsgemeinschaft; DFG Schu 95/9-1 and SFB 418

short-time dynamic scaling, the static exponents β and ν as well as the critical temperature T_c are also extracted from the numerical data.

The Hamiltonian of the FFFXY model on a square lattice can be written as

$$H = -K \sum_{\langle ij \rangle} \cos(\theta_i - \theta_j + A_{ij}), \quad (3)$$

In our notation the factor $1/kT$ has been absorbed in the coupling K , θ_i is the angle of the spin (a unit vector) located on site i , A_{ij} determine the frustration and the sum is over the nearest neighbours. A simple realization of the FFFXY model is by taking $A_{ij} = \pi$ on half of the vertical links and $A_{ij} = 0$ on other links. This is shown in Fig. 1, where the links with $A_{ij} = \pi$ are marked by dotted lines. The spin configuration of one ground state of the model is also shown in Fig. 1. The order parameter for the second order phase transition is the staggered chiral magnetization defined as [19]

$$M_I = \left\langle \frac{1}{L^2} \sum_r (-1)^{r_x + r_y} \operatorname{sgn} \left[\sum_{\langle ij \rangle \in P_r} \sin(\theta_i - \theta_j + A_{ij}) \right] \right\rangle \quad (4)$$

where (r_x, r_y) is the coordinate of the plaquette P_r .

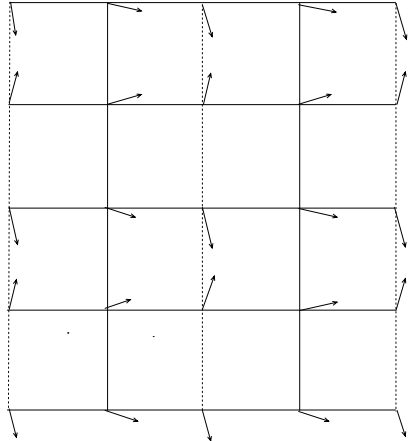


FIG. 1. One of the ground states of the FFFXY model. Dotted lines denote the links with $A_{ij} = \pi$.

At first, we investigate the short-time critical behaviour of M_I in the dynamic process starting from an initial state with a very high temperature and a small magnetization m_0 . We prepare an initial configuration in the following way: first we randomly generate all spins

on the lattice, then we randomly choose a number of plaquettes and orient their spins according to the configuration of the ground state shown in Fig. 1 till the initial magnetization m_0 is achieved. After the initial configuration is generated, the system is released to the dynamic evolution with the Metropolis algorithm at temperatures around T_c . We have performed our simulation on lattices of size $L = 128$ and 256 , and updated the system up to 1000 Monte Carlo steps. The average is taken over independent initial configurations with 40 000 samples for $L = 128$ and 10 000 samples for $L = 256$. Errors are estimated by dividing the samples into three groups.

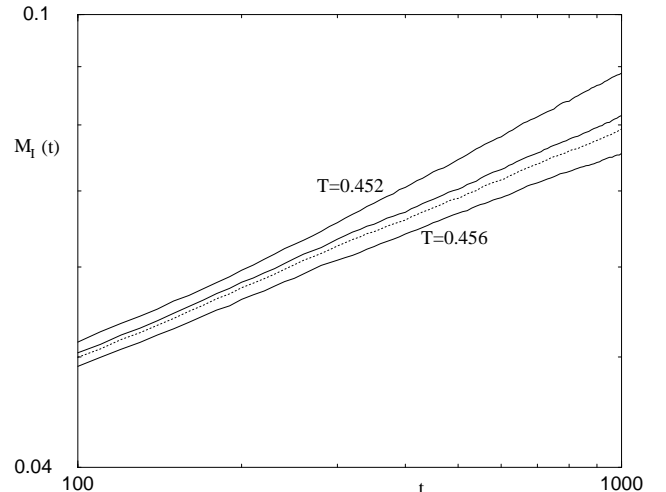


FIG. 2. The time evolution of the chiral magnetization $M_I(t)$ when starting from a disordered initial state. The temperatures are $T = 0.452, 0.454$, and 0.456 from above. The dotted line represents the magnetization at $T_c = 0.4547$.

In order to locate the critical temperature T_c , simulations have been carried out with three temperatures $T = 0.452, 0.454$ and 0.456 . The initial magnetization is set to $m_0 = 0.06$. In Fig. 2, the time evolution of the magnetization $M_I(t)$ at different temperatures is plotted with solid lines in log-log scale for the lattice size $L = 128$. Data within the microscopic time scale $t_{mic} \sim 100$, which are dependent on microscopic details, are not included. Indeed we observe that the magnetization increases at the macroscopic early time. The magnetization at the temperature between $T = 0.452$ and 0.456 can be obtained by quadratic interpolation. From the scaling form (1) and as suggested in Ref. [9], searching for a curve $M_I(t)$ with the best power law behaviour can yield an estimate of the critical temperature. In Fig. 2, the dotted line represents such a curve and the corresponding critical temperature $T_c = 0.4547(8)$. From the slope of this curve, the exponent $\theta = 0.200(3)$ is obtained.

From an analysis of the data for $L = 256$ we have observed that the finite size effect for $L = 128$ is already

sufficiently small to be neglected. In fact, the finite size effect can easily be controlled in the short-time dynamics, and this is an advantage of the short-time dynamic approach. On the other hand, the critical exponent θ is defined in the limit $m_0 \rightarrow 0$. Therefore, the finite m_0 effect should also be considered. However, within statistical errors our data for $m_0 = 0.04$ and $m_0 = 0.06$ show no difference. Hence the finite m_0 effect will also be ignored.

In principle, other static and dynamic critical exponents can be obtained from $\partial_\tau \ln M_I$, the second moment and the fourth moment of the magnetization, the auto-correlation and other observables. For example,

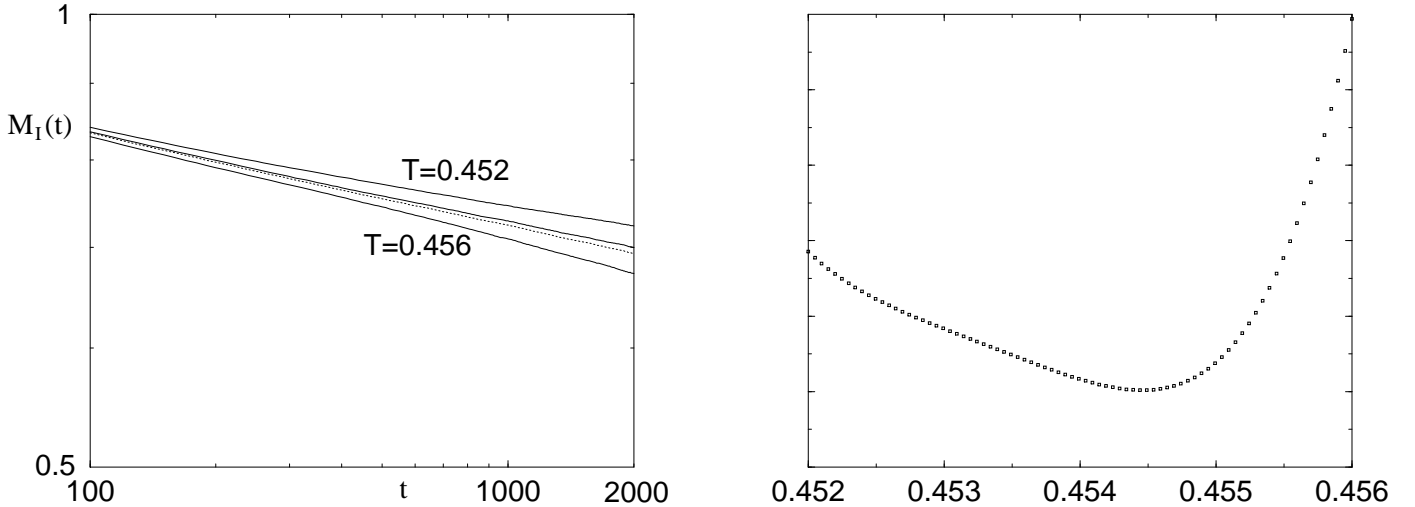


FIG. 3. (a) The time evolutions of the chiral magnetizations $M_I(t)$ when starting from an ordered state. From above, the solid lines represent the $M_I(t)$ at $T=0.452$, 0.454 , and 0.456 . The dotted line is the magnetization at the critical temperature $T_c = 0.4545$. (b) Deviation of $M_I(t)$ from the power law behaviour within the time interval $[200, 1000]$.

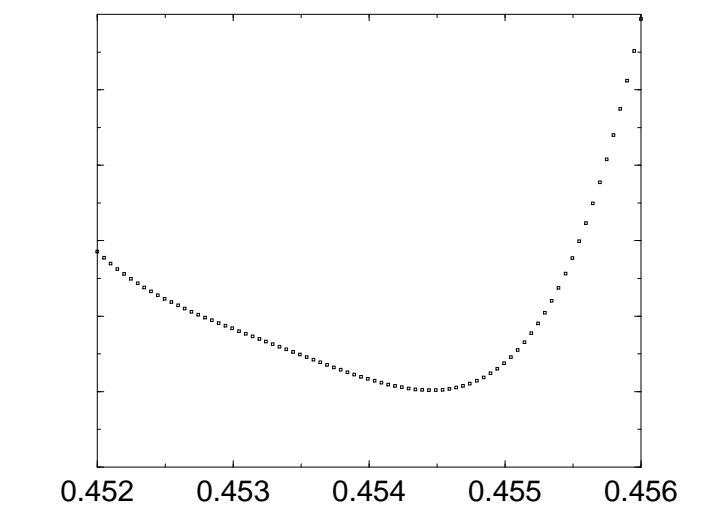
The estimation of T_c can now be performed again. From the scaling form (2) and for sufficiently large L we can easily deduce the scaling behaviour for the magnetization ($k = 1$)

$$M_I(t, \tau) = t^{-\beta/\nu z} G(t^{1/\nu z} \tau). \quad (5)$$

At the critical temperature, $\tau = 0$, M_I undergoes a power law decay. When $\tau \neq 0$ this power law is modified by the scaling function $G(t^{1/\nu z} \tau)$. As pointed out earlier, the temperature for which the magnetization has the best power law behaviour is the critical temperature T_c . In Fig. 3 (a), the time evolution of $M_I(t)$ at $T = 0.452$, 0.454 and 0.456 is plotted in log-log scale. $M_I(t)$ at other temperatures in the interval $[0.452, 0.456]$ can be estimated by a quadratic interpolation. To avoid the effect of t_{mic} , measurements are performed in the time interval $[200, 2000]$. The deviation from the power law can be estimated in different ways, e.g. as described in Ref.

$1/\nu z = 0.59(3)$ is obtained from $\partial_\tau \ln M_I(t, \tau)|_{\tau=0}$. However, this dynamic process starting from a disordered state is not the best choice to obtain these exponents or the critical temperature T_c . A dynamic process starting from an ordered state is preferable, since the fluctuation is weaker.

For this purpose, simulations were also performed with temperatures $T = 0.452$, 0.454 and 0.456 , starting from an ordered initial state. The lattice size chosen was $L = 256$ and the system was updated for 2000 Monte Carlo steps. The average was taken over 2000 samples. The ordered initial state was taken to be the ground state shown in Fig. 1.



[9]. In this paper, we choose to measure the deviation as the error by fitting $M_I(t)$ directly to a power law in the time interval $[200, 2000]$. Furthermore we perform the fitting in log scale, i.e. less weight is given to the data in the longer time regime. In Fig. 3 (b), the deviation of M_I from the power law is plotted as a function of the temperature. The clear minimum confidently indicates the critical temperature T_c . The resulting value $T_c = 0.4545(2)$ is consistent with $T_c = 0.4547(8)$ obtained from Fig. 2 and very close to those values ranging from $T_c = 0.451$ to 0.454 reported in most of the recent references [17,18,21,22]. Our statistical error, however, is smaller. The corresponding magnetization is also plotted in Fig. 3 (a) with a dotted line. The slope of this curve yields the critical exponent $\beta/\nu z = 0.0602(2)$. The quality of this measurement is very good. With β/ν given, one can obtain a rigorous z or vice versa [10,26,11,9,6]. As compared to simulations with a disordered initial state, the measurements here carry much less fluctuations.

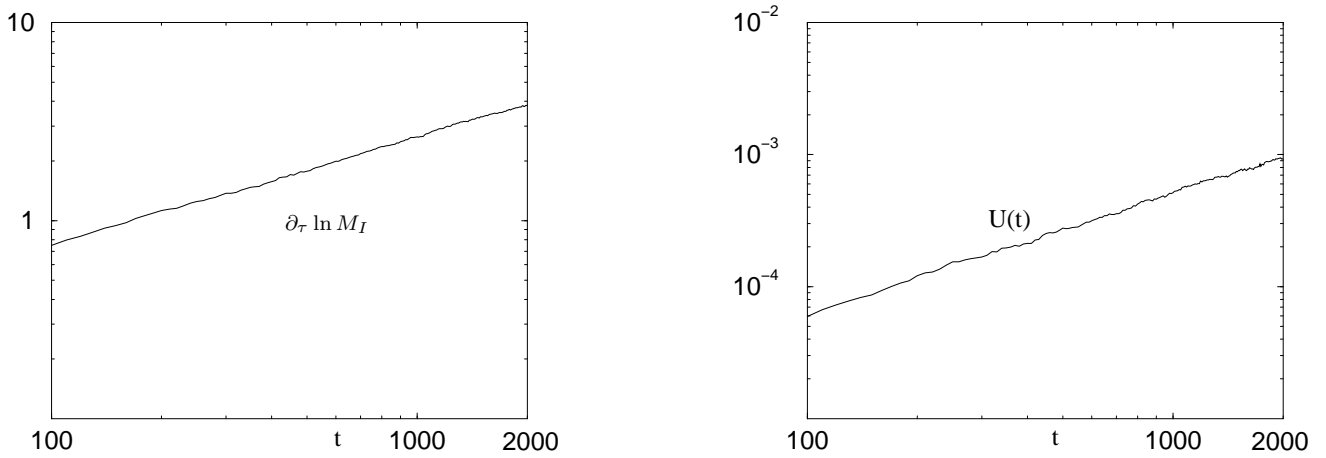


FIG. 4. (a) The derivative $\partial_\tau \ln M_I(t, \tau)|_{\tau=0}$ plotted versus time in log-log scale. (b) The time-dependent Binder cumulant U .

To extract the critical exponent $1/\nu z$, differentiation of Eq. (5) leads to

$$\partial_\tau \ln M_I(t, \tau)|_{\tau=0} = t^{1/\nu z} \partial_\tau \ln G(\tau')|_{\tau'=0}. \quad (6)$$

Therefore, $\partial_\tau \ln M_I(t, \tau)|_{\tau=0}$ should also present a power law behaviour in the beginning of the time evolution. In Fig. 4 (a), $\partial_\tau \ln M_I(t, \tau)$ at $T_c = 0.4545$ is plotted in log-log scale. The power law behaviour is clearly seen. The slope yields the critical exponent $1/\nu z = 0.57(1)$.

The final step is to seek the dynamical critical exponent z . For this, we introduce a time-dependent Binder

cumulant $U(t, L) = M_I^{(2)}/M_I^2 - 1$. Due to the short spatial correlation length in the short-time regime, a simple finite size scaling analysis shows at the critical temperature

$$U(t, L) \sim t^{d/z}. \quad (7)$$

In Fig. 4 (b), the curve for $U(t, L)$ in log-log scale shows a nice power law behaviour. The slope gives the critical exponent $d/z = 0.92(2)$. Table I summarizes the results. The errors in the measurements from $m_0 = 1$ are clearly smaller than those from $m_0 = 0.06$.

	T_c	θ	$\beta/\nu z$	$1/\nu z$	d/z
$m_0 = 1$	0.4545(2)		0.0602(2)	0.57(1)	0.92(2)
$m_0 = 0.06$	0.4547(8)	0.200(3)		0.59(3)	

TABLE I. The critical temperature and the critical exponents measured by simulations starting from an ordered as well as a disordered state.

	This work	Ref. [22] (1996)	Ref. [21] (1995)	Ref. [18] (1994)	Ref. [17] (1993)	Ising
T_c	0.4545(2)	0.451(1)	0.452(1)	0.454(2)	0.454(3)	
ν	0.81(2)	0.898(3)	1	0.813(5)	0.80(5)	1
$2\beta/\nu$	0.261(5)			0.22(2)	0.38(2)	0.25
z	2.17(4)					2.165(10)
θ	0.202(3)					0.191(3)

TABLE II. Critical exponents obtained in this work and values reported in some recent references. Reference [21] does not provide an estimate of the error on $\nu = 1$. For the Ising model, exponents ν and $2\beta/\nu$ are exact values and θ is taken from Refs. [8,27]. The exponent z in the literature ranges from 2.155 to 2.172 [6,26,8,27]. Here an ‘average’ value is given.

The interesting and important property of the Binder cumulant is that one can estimate independently the dynamic exponent z . With z in hand, we calculate the critical exponents $2\beta/\nu$ and ν from $\beta/\nu z$ and $1/\nu z$. Table II lists all critical exponents along with the results reported in the recent literature. Now $\theta = 0.202(3)$ is measured at $T_c = 0.4545$, which shows a small difference from that at $T = 0.4547$. Our short-time dynamic measurements support those from Ref. [18] and provide extra new results for the dynamic exponents z and θ . The exponent ν of the FFFXY model is different from that of the Ising model by nearly 20 per cent. This indicates that the chiral degree of freedom of the FFFXY model is in a new universality class. Other exponents of the FFFXY model do not differ much from those of the Ising model. From our numerical data, we observe that the values of the critical exponents are rather sensitive to the assumed or measured critical temperature T_c . This should be one of the main reasons for the different values of the exponents reported in the literature. Figure 2 and, in particular, Fig. 3, give us confidence in our measurements of the critical temperature T_c . Furthermore, our exponent ν is extracted from the data in the close neighbourhood of T_c , in contrast to many simulations in equilibrium. The finite size effect is also well under control in the short-time dynamic approach.

In conclusions, using Monte Carlo methods, we have systematically investigated and confirmed the universal short-time dynamic behaviour of the second order phase transition in the two-dimensional fully frustrated XY model. Based on the short-time dynamic scaling form, all static and dynamical critical exponents are determined. The dynamic exponents θ and z are obtained for the first time and the measurement of the exponent $\beta/\nu z$ and the critical temperature T_c is very precise. The estimated value $\nu = 0.81(2)$ is clearly different from $\nu = 1$ for the Ising model. Our investigation of the chiral degree of freedom of the FFFXY model is to date the most systematic. We are convinced that the short-time dynamic approach is not only conceptually interesting but also practically efficient. In the simulations we do not encounter difficulties associated with large correlation times since our measurements are carried out in the short-time regime and we do not have the problem of generating independent configurations.

A possible extension of the present work is the Kosterlitz-Thouless phase transition. In fact, some exponents have been obtained [28,29]. However, owing to the absence of symmetry breaking, a clear signal such as in Fig. 3 does not exist for the Kosterlitz-Thouless transition temperature T_{KT} . The determination of T_{KT} and of the exponent ν is very difficult and requires extensive simulations and a careful analysis.

- [1] H. K. Janssen, B. Schaub and B. Schmittmann, *Z. Phys. B* **73** (1989) 539.
- [2] D. A. Huse, *Phys. Rev. B* **40** (1989) 304.
- [3] K. Humayun and A. J. Bray, *J. Phys. A* **24** (1991) 1915.
- [4] Z.B. Li, U. Ritschel and B. Zheng, *J. Phys. A: Math. Gen.* **27** (1994) L837.
- [5] L. Schülke and B. Zheng, *Phys. Lett. A* **204** (1995) 295.
- [6] B. Zheng, *Monte Carlo Simulations of Short-time Critical Dynamics*, Halle Univ., 1998, review article, to be published in *Int. J. Mod. Phys. B*.
- [7] P.C. Hohenberg and B.I. Halperin, *Rev. Mod. Phys.* **49** (1977) 435.
- [8] P. Grassberger, *Physica A* **214** (1995) 547.
- [9] L. Schülke and B. Zheng, *Phys. Lett. A* **215** (1996) 81.
- [10] D. Stauffer, *Physica A* **186** (1992) 197.
- [11] D. Stauffer and R. Knecht, *Int. J. Mod. Phys. C* **7** (1996) 893.
- [12] Z.B. Li, L. Schülke and B. Zheng, *Phys. Rev. E* **53** (1996) 2940.
- [13] R. E. Blundell, K. Humayun and A. J. Bray, *J. Phys. A, Math. Gen.* **25** (1992) L733.
- [14] J. Lee, J.M. Kosterlitz and E. Granato, *Phys. Rev. B* **43** (1991) 11531.
- [15] D.B. Nicolaides, *J. Phys. A* **24** (1991) L231.
- [16] G. Ramirez-Santiago and J. José, *Phys. Rev. Lett.* **68** (1992) 1224.
- [17] E. Granato and M. P. Nightingal, *Phys. Rev. B* **48** (1993) 7438.
- [18] S. Lee and K. Lee, *Phys. Rev. B* **49** (1994) 15184.
- [19] G. Ramirez-Santiago and J.V. José, *Phys. Rev. B* **49** (1994) 9567.
- [20] S. J. Lee, J. R. Lee and B. Kim, *Phys. Rev. E* **51** (1995) R4.
- [21] P. Olsson, *Phys. Rev. Lett.* **75** (1995) 2758.
- [22] J. V. José and G. Ramirez-Santiago, *Phys. Rev. Lett.* **77** (1996) 4849.
- [23] P. Olsson, *Phys. Rev. Lett.* **77** (1996) 4850.
- [24] P. Olsson, *Phys. Rev. B* **55** (1997) 3585.
- [25] G. S. Jeon, S. Y. Park and M. Y. Choi, *Phys. Rev. B* **55** (1997) 14088.
- [26] N. Ito, *Physica A* **196** (1993) 591.
- [27] K. Okano, L. Schülke, K. Yamagishi and B. Zheng, *Nucl. Phys. B* **485** (1997) 727.
- [28] H.J. Luo and B. Zheng, *Mod. Phys. Lett. B* **11** (1997) 615.
- [29] H.J. Luo, L. Schülke and B. Zheng, *Universal Short-time Behaviour of the Dynamic Fully Frustrated XY Model*, to be published in *Phys. Rev. E*, cond-mat/9705222, 1997.